
PDE-Net: Learning PDEs from Data

Zichao Long^{* 1} Yiping Lu^{* 1} Xianzhong Ma^{* 1 2} Bin Dong^{3 4 5}

Abstract

Partial differential equations (PDEs) play a prominent role in many disciplines of science and engineering. PDEs are commonly derived based on empirical observations. However, with the rapid development of sensors, computational power, and data storage in the past decade, huge quantities of data can be easily collected and efficiently stored. Such vast quantity of data offers new opportunities for data-driven discovery of physical laws. Inspired by the latest development of neural network designs in deep learning, we propose a new feed-forward deep network, called PDE-Net, to fulfill two objectives at the same time: to accurately predict dynamics of complex systems and to uncover the underlying hidden PDE models. Comparing with existing approaches, our approach has the most flexibility by learning both differential operators and the nonlinear response function of the underlying PDE model. A special feature of the proposed PDE-Net is that all filters are properly constrained, which enables us to easily identify the governing PDE models while still maintaining the expressive and predictive power of the network. These constraints are carefully designed by fully exploiting the relation between the orders of differential operators and the orders of sum rules of filters (an important concept originated from wavelet theory). Numerical experiments show that the PDE-Net has the potential to uncover the hidden PDE of the observed dynamics, and predict the dynamical behavior for a relatively long time, even in a noisy environment.

1. Introduction

Differential equations, especially partial differential equations (PDEs), play a prominent role in many disciplines to describe the governing physical laws underlying a given system of interest. Traditionally, PDEs are derived based on simple physical principles such as conservation laws, minimum energy principles, or based on empirical observations. Important examples include the Navier-Stokes equations in fluid dynamics, the Maxwell's equations for electromagnetic propagation, and the Schrödinger's equations in quantum mechanics. However, many complex systems in modern applications (such as many problems in climate science, neuroscience, finance, etc.) still have eluded mechanisms, and the governing equations of these systems are only partially known. With the rapid development of sensors, computational power, and data storage in the last decade, huge quantities of data can be easily collected and efficiently stored. Such vast quantity of data offers new opportunities for data-driven discovery of potentially new physical laws. Then, one may ask the following interesting and intriguing question: can we learn a PDE model (if there exists one) from a given data set and perform accurate and efficient predictions using the learned model?

1.1. Related Work

Earlier attempts on data-driven discovery of hidden physical laws include (Bongard & Lipson, 2007; Schmidt & Lipson, 2009). Their main idea is to compare numerical differentiations of the experimental data with analytic derivatives of candidate functions, and apply the symbolic regression and the evolutionary algorithm to determining the nonlinear dynamical system. Recently, (Brunton et al., 2016), (Schaeffer, 2017), (Rudy et al., 2017) and (Wu & Zhang, 2017) proposed an alternative approach using sparse regression. They constructed a dictionary of simple functions and partial derivatives that were likely to appear in the unknown governing equations. Then, they took advantage of sparsity promoting techniques to select candidates that most accurately represent the data. When the form of the nonlinear response of a PDE is known, except for some scalar parameters, (Raissi & Karniadakis, 2017) presented a framework to learn these unknown parameters by introducing regularity between two consecutive time step using Gaussian process. (de Bezenac et al., 2017) studied the problem of sea surface

^{*}Equal contribution ¹School of Mathematical Sciences, Peking University, Beijing, China ²Beijing Computational Science Research Center, Beijing, China ³Beijing International Center for Mathematical Research, Peking University, Beijing, China ⁴Center for Data Science, Peking University ⁵Laboratory for Biomedical Image Analysis, Beijing Institute of Big Data Research. Correspondence to: Bin Dong <dongbin@math.pku.edu.cn>.

temperature prediction (SSTP). They assumed that the underlying physical model is an advection-diffusion equation. They designed a special neural network according to the general solution of advection-diffusion equations. Comparing with traditional numerical methods, their approach showed improvements in accuracy and decrease in computational time.

These recent work greatly advanced the progress of the problem. However, symbolic regression is computationally expensive and does not scale very well to large systems. The sparse regression method requires to fix certain numerical approximations of the spatial differentiations in the dictionary beforehand, which limits the expressive and predictive power of the dictionary. Although the framework presented by Raissi & Karniadakis (2017); Raissi et al. (2017) is able to learn hidden physical laws using less data than the approach of sparse regression, the explicit form of the PDEs is assumed to be known except for a few scalar learnable parameters. The approach of de Bezenac et al. (2017) is specifically designed for advection-diffusion equations, and cannot be readily extended to other types of equations. Therefore, extracting governing equations from data in a less restrictive setting remains a great challenge.

The main objective of this paper is to accurately predict the dynamics of complex systems and to uncover the underlying hidden PDE models (should they exist) at the same time, with minimal prior knowledge on the systems. Our inspiration comes from the latest development of deep learning techniques in computer vision. An interesting fact is that some popular networks in computer vision, such as ResNet(He et al., 2016a;b), have close relationship with PDEs (Chen et al., 2015; E, 2017; Haber & Ruthotto, 2017; Sonoda & Murata, 2017; Lu et al., 2018; Chang et al., 2018). However, existing deep networks designed in deep learning mostly emphasis on expressive power and prediction accuracy. These networks are not transparent enough to be able to reveal the underlying PDE models, although they may perfectly fit the observed data and perform accurate predictions. Therefore, we need to carefully design the network by combining knowledge from deep learning and applied mathematics so that we can learn the governing PDEs of the dynamics and make accurate predictions at the same time.

1.2. Our Approach

In this paper, we design a deep feed-forward network, named PDE-Net, based on the following generic nonlinear evolution PDE

$$u_t = F(x, u, \nabla u, \nabla^2 u, \dots), \quad x \in \Omega \subset \mathbb{R}^2, \quad t \in [0, T].$$

The objective of the PDE-Net is to learn the form of the nonlinear response F and to perform accurate predictions. Unlike the existing work, the proposed network only requires

minor knowledge on the form of the nonlinear response function F , and requires no knowledge on the involved differential operators (except for their maximum possible order) and their associated discrete approximations. The nonlinear response function F can be learned using neural networks or other machine learning methods, while discrete approximations of the differential operators are learned using convolution kernels (i.e. filters) jointly with the learning of the response function F . If we have a prior knowledge on the form of the response function F , we can easily adjust the network architecture by taking advantage of the additional information. This may simplify the training and improve the results.

A particular novelty of our approach is that we impose appropriate constraints on the learnable filters in order to easily identify the governing PDE models while still maintaining the expressive and predictive power of the network. This makes our approach different from existing deep convolutional networks which mostly emphasis on the prediction accuracy of the networks, as well as all the existing approaches of learning PDEs from data which assume either the form of the response function is known or have fixed approximations of the differential operators. In other words, our proposed approach not only has vast flexibility in fitting observed dynamics and is able to accurately predict its future behavior, but is also able to reveal the hidden equations driving the observed dynamics.

2. PDE-Net: A Flexible Deep Architecture to Learn PDEs from Data

Given a series of measurements of some physical quantities $\{u(t, \cdot) : t = t_0, t_1, \dots\}$ on the spatial domain $\Omega \subset \mathbb{R}^2$, with $u(t, \cdot) : \Omega \mapsto \mathbb{R}$, we want to discover the governing PDEs of the data. We assume that the observed data are associated with a PDE that takes the following general form:

$$u_t(t, x, y) = F(x, y, u, u_x, u_y, u_{xx}, u_{xy}, u_{yy}, \dots), \quad (1)$$

where $(x, y) \in \Omega \subset \mathbb{R}^2, t \in [0, T]$. Our objective is to design a feed-forward network, named the PDE-Net, that approximates the PDE (1) in the way that: 1) we can predict the dynamical behavior of the equation for as long time as possible; 2) we are able to reveal the form of the response function F and the differential operators involved. There are two main components of the PDE-Net that are combined together in the same network: one is automatic determination on the differential operators involved in the PDE and their discrete approximations; the other is to approximate the nonlinear response function F . In this section, we start with discussions on the relation between convolutions and differentiations in discrete setting.

2.1. Convolutions and Differentiations

A profound relationship between convolutions and differentiations was presented by Cai et al. (2012); Dong et al. (2017), where the authors discussed the connection between the order of sum rules of filters and the orders of differential operators. Note that the order of sum rules is closely related to the order of vanishing moments in wavelet theory (Daubechies, 1992; Mallat, 1999). We first recall the definition of the order of sum rules.

Definition 2.1 (Order of Sum Rules). *For a filter q , we say q to have sum rules of order $\alpha = (\alpha_1, \alpha_2)$, where $\alpha \in \mathbb{Z}_+^2$, provided that*

$$\sum_{k \in \mathbb{Z}^2} k^\beta q[k] = 0 \quad (2)$$

for all $\beta = (\beta_1, \beta_2) \in \mathbb{Z}_+^2$ with $|\beta| := \beta_1 + \beta_2 < |\alpha|$ and for all $\beta \in \mathbb{Z}_+^2$ with $|\beta| = |\alpha|$ but $\beta \neq \alpha$. If (2) holds for all $\beta \in \mathbb{Z}_+^2$ with $|\beta| < K$ except for $\beta \neq \beta$ with certain $\beta \in \mathbb{Z}_+^2$ and $|\beta| = J < K$, then we say q to have total sum rules of order $K \setminus \{J + 1\}$.

In practical implementation, the filters are normally finite and can be understood as matrices. For an $N \times N$ filter q (N is an odd number), assuming the indices of q start from $-\frac{N-1}{2}$, (2) can be written in the following simpler form

$$\sum_{l=-\frac{N-1}{2}}^{\frac{N-1}{2}} \sum_{m=-\frac{N-1}{2}}^{\frac{N-1}{2}} l^{\beta_1} m^{\beta_2} q[l, m] = 0.$$

The following proposition from Dong et al. (2017) links the orders of sum rules with orders of differential operator.

Propositin 2.1. *Let q be a filter with sum rules of order $\alpha \in \mathbb{Z}_+^2$. Then for a smooth function $F(x)$ on \mathbb{R}^2 , we have*

$$\frac{1}{\varepsilon^{|\alpha|}} \sum_{k \in \mathbb{Z}^2} q[k] F(x + \varepsilon k) = C_\alpha \frac{\partial^\alpha}{\partial x^\alpha} F(x) + O(\varepsilon), \text{ as } \varepsilon \rightarrow 0. \quad (3)$$

If, in addition, q has total sum rules of order $K \setminus \{|\alpha| + 1\}$ for some $K > |\alpha|$, then

$$\frac{1}{\varepsilon^{|\alpha|}} \sum_{k \in \mathbb{Z}^2} q[k] F(x + \varepsilon k) = C_\alpha \frac{\partial^\alpha}{\partial x^\alpha} F(x) + O(\varepsilon^{K-|\alpha|}), \text{ as } \varepsilon \rightarrow 0. \quad (4)$$

According to Proposition 2.1, an α th order differential operator can be approximated by the convolution of a filter with α order of sum rules. Furthermore, according to (4), one can obtain a high order approximation of a given differential operator if the corresponding filter has an order of total sum rules with $K > |\alpha| + k, k \geq 1$. For example, consider filter

$$q = \begin{pmatrix} 1 & 0 & -1 \\ 2 & 0 & -2 \\ 1 & 0 & -1 \end{pmatrix}. \text{ It has a sum rules of order } (1, 0),$$

and a total sum rules of order $3 \setminus \{2\}$. Thus, up to a constant

and a proper scaling, q corresponds to a discretization of $\frac{\partial}{\partial x}$ with second order approximation.

Now, we introduce the concept of *moment matrix* for a given filter that will be used to constrain filters in the PDE-Net. For an $N \times N$ filter q , define the moment matrix of q as

$$M(q) = (m_{i,j})_{N \times N}, \quad (5)$$

where $m_{i,j} = \frac{1}{(i-1)!(j-1)!} \sum_{k \in \mathbb{Z}^2} k_1^{i-1} k_2^{j-1} q[k_1, k_2]$, for $i, j = 1, 2, \dots, N$. We shall call the (i, j) -element of $M(q)$ the $(i-1, j-1)$ -moment of q for simplicity. Combining (5) and Proposition 2.1, one can easily see that filter q can be designed to approximate any differential operator at any given approximation order by imposing constraints on $M(q)$. For example, if we want to approximate $\frac{\partial u}{\partial x}$ (up to a constant) by convolution $q \otimes u$ where q is a 3×3 filter, we can consider the following constrains on $M(q)$:

$$\begin{pmatrix} 0 & 0 & \star \\ 1 & \star & \star \\ \star & \star & \star \end{pmatrix} \quad \text{or} \quad \begin{pmatrix} 0 & 0 & 0 \\ 1 & 0 & \star \\ 0 & \star & \star \end{pmatrix}. \quad (6)$$

Here, \star means no constraint on the corresponding entry. The constraints described by the moment matrix on the left of (6) guarantee the approximation accuracy is at least first order, and the ones on the right guarantee an approximation of at least second order. In particular, when all entries of

$M(q)$ are constrained, e.g. $M(q) = \begin{pmatrix} 0 & 0 & 0 \\ 1 & 0 & 0 \\ 0 & 0 & 0 \end{pmatrix}$, the

corresponding filter can be uniquely determined, in which case we call it a “frozen” filter. In the PDE-Net which shall be introduced in the next subsection, all filters are learned subjected to partial constraints on their associated moment matrices. It is worth noting that the approximation property of a filter is limited by its size. Generally speaking, large filters can approximate higher order differential operators or lower order differential operators with higher approximation orders. However, larger filters lead to more memory overhead and higher computation cost. It is a wisdom to balance the trade-off in practice.

2.2. Architecture of PDE-Net

Given the evolution PDE (1), we consider forward Euler as the temporal discretization. One may consider more sophisticated temporal discretization which leads to different network architectures. For simplicity, we focus on forward Euler in this paper.

ONE δt -BLOCK:

Let $\tilde{u}(t_{i+1}, \cdot)$ be the predicted value of u at time t_{i+1} based on the value of u at t_i . Then, we have

$$\tilde{u}(t_{i+1}, \cdot) = D_0 u(t_i, \cdot) + \Delta t \cdot F(x, y, D_{00} u, D_{10} u, D_{01} u, D_{20} u, \dots). \quad (7)$$

Here, the operators D_0 and D_{ij} are convolution operators with the underlying filters denoted by q_0 and q_{ij} , i.e. $D_0 u = q_0 \otimes u$ and $D_{ij} u = q_{ij} \otimes u$. The operators D_{10} , D_{01} , D_{11} , etc. approximate differential operators, i.e. $D_{ij} u \approx \frac{\partial^{i+j} u}{\partial^i x \partial^j y}$. The operators D_0 and D_{00} are spatial average operators. The purpose of introducing these average operators in stead of using the identity is to improve the expressive power of the network and enables it to capture more complex dynamics. Other than the assumption that the observed dynamics is governed by a PDE of the form (1), we assume that the highest order of the PDE is less than some positive integer. Then, the task of approximating F is equivalent to a multivariate regression problem, which can be approximated by a point-wise neural network (with shared weights across the computation domain Ω) or other classical machine learning methods. Combining the approximation of differential operators and the nonlinear function F , we achieve an approximation framework of (7) which will be referred to as a δt -block (see Figure 1).

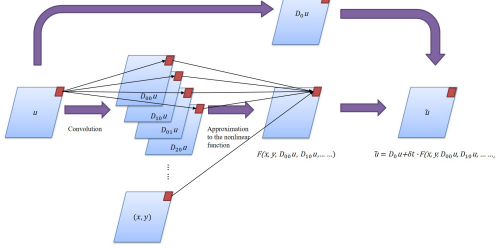


Figure 1. The schematic diagram of a δt -block.

PDE-NET (MULTIPLE δt -BLOCKS):

One δt -block only guarantees the accuracy of one-step dynamics, which does not take error accumulation into consideration. In order to facilitate a long-term prediction, we stack multiple δt -blocks into a deep network, and call this network the *PDE-Net* (see Figure 2). The importance of stacking multiple δt -blocks will be demonstrated in Section 3.

The PDE-Net can be easily described as: (1) stacking one δt -block multiple times; (2) sharing parameters in all δt -blocks. Given an input data $u(t_i, \cdot)$, training a PDE-Net with n δt -blocks needs to minimize the accumulated error $\|u(t_{i+n}, \cdot) - \tilde{u}(t_{i+n}, \cdot)\|_2^2$, where $\tilde{u}(t_{i+n}, \cdot)$ is the output from the PDE-Net (i.e. n δt -blocks) with input $u(t_i, \cdot)$.

LOSS FUNCTION AND CONSTRAINTS:

Consider the data set $\{u_j(t_i, \cdot) : i, j = 0, 1, \dots\}$, where j indicates the j -th solution path with a certain initial condition of the unknown dynamics. We would like to train the PDE-Net with n δt -blocks. For a given $n \geq 1$, every pair of the data $\{u_j(t_i, \cdot), u_j(t_{i+n}, \cdot)\}$, for each i and j , is a training sample, where $u_j(t_i, \cdot)$ is the input and $u_j(t_{i+n}, \cdot)$

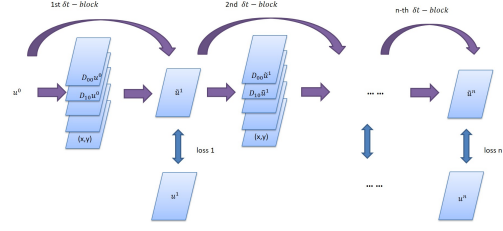


Figure 2. The schematic diagram of the PDE-Net.

is the label that we need to match with the output from the PDE-Net. We select the following simple ℓ_2 loss function for training:

$$L = \sum_{i,j} l_{ij}, \text{ where } l_{ij} = \|u_j(t_{i+n}, \cdot) - \tilde{u}_j(t_{i+n}, \cdot)\|_2^2,$$

where $\tilde{u}_j(t_{i+n}, \cdot)$ is the output of the PDE-Net with $u_j(t_i, \cdot)$ as the input.

All the filters involved in the PDE-Net are properly constrained using their associated moment matrices. Let q_0 and q_{ij} be the underlying filters of D_0 and D_{ij} . We impose the following constraints

$$(M(q_0))_{1,1} = 1, \quad (M(q_{00}))_{1,1} = 1,$$

and for $i + j > 0$, we set

$$(M(q_{i,j}))_{k_1, k_2} = 0, k_1 + k_2 \leq i + j + 2, (k_1, k_2) \neq (i + 1, j + 1);$$

$$(M(q_{i,j}))_{i+1, j+1} = 1.$$

To demonstrate the necessity of learnable filters, we will compare the PDE-Net having the aforementioned constraints on the filters with the PDE-Net having frozen filters. To differentiate the two cases, we shall call the PDE-Net with frozen filters “the Frozen-PDE-Net”.

NOVELTY OF THE PDE-NET:

Different from fixing numerical approximations of differentiations in advance in sparse regression methods (Schaeffer, 2017; Rudy et al., 2017), using learnable filters makes the PDE-Net more flexible, and enables more robust approximation of unknown dynamics and longer time prediction (see numerical experiments in Section 3 and Section 4). Furthermore, the specific form of the response function F is also approximated from the data, rather than assumed to be known in advance (such as (Raissi & Karniadakis, 2017; Raissi et al., 2017)). On the other hand, by inflicting constraints on moment matrices, we can identify which differential operators are included in the underlying PDE which helps with identifying the nonlinear response function F . This grants transparency to the PDE-Net and the potential to reveal hidden physical laws. Therefore, the proposed PDE-Net is distinct from the existing learning based method to discover PDEs from data, as well as networks designed in deep learning for computer vision tasks.

2.3. Initialization and training

In the PDE-Net, parameters can be divided into three groups: 1) filters to approximate differential operators; 2) the parameters of the point-wise neural network to approximate F ; and 3) hyper-parameters, such as the number of filters, the size of filters, the number of layers, etc. The parameters of the point-wise neural network are shared across the computation domain Ω , and are initialized by random sampling from a Gaussian distribution. For the filters, we initialize them by freezing them to their corresponding differential operators.

Instead of training an n -layer PDE-Net directly, we adopt layer-wise training, which improves the training speed. Details on training can be found in (Long et al., 2018). All the parameters in each of the δt -block are shared across layers. In addition, we add a warm-up step before the training of the first δt -block. The warm-up step is to obtain a good initial guess of the parameters of the point-wise neural network that approximates F by using frozen filters.

2.4. Relations to some existing networks

In recent years, a variety of deep neural networks have been introduced with great success in computer vision. The structure of the proposed PDE-Net is similar to some existing networks such as the Network-In-Network (NIN) (Lin et al., 2013) and the deep Residual Neural Network (ResNet) (He et al., 2016a;b).

The NIN is an improvement over the traditional convolutional neural networks. One of the special designs of NIN is the use of multilayer perceptron convolution (mlpconv) layers instead of the ordinary convolution layers. An mlpconv layer contains the convolutions and small point-wise neural networks. Such design can improve the ability of the network to extract nonlinear features from shallow layers. The inner structure of one δt -block of the PDE-Net is similar to the mlpconv layer, and the multiple δt -blocks structure is similar to the NIN structure, except for the pooling and ReLU operations.

On the other hand, each δt -block of the PDE-Net has two paths (see Figure 1 and Figure 2): one is for the averaged quantity of u and the other is for the increment F . This structure coincides with the “residual block” introduced in ResNet. In fact, there has been a substantial study on the relation between ResNet and dynamical systems recently (E, 2017; Haber & Ruthotto, 2017; Sonoda & Murata, 2017).

3. Numerical Studies: Convection-Diffusion Equations

Convection-diffusion equations are classical PDEs that are used to describe physical phenomena where particles, en-

ergy, or other physical quantities are transferred inside a physical system due to two processes: diffusion and convection (Chandrasekhar, 1943).

3.1. Simulated data, training and testing

We consider a 2-dimensional linear variable-coefficient convection-diffusion equation on $\Omega = [0, 2\pi] \times [0, 2\pi]$,

$$\begin{cases} \frac{\partial u}{\partial t} &= a(x, y)u_x + b(x, y)u_y + 0.2u_{xx} + 0.3u_{yy}, \\ u|_{t=0} &= u_0(x, y), \end{cases} \quad (8)$$

with $(t, x, y) \in [0, 0.3] \times \Omega$, where

$$\begin{aligned} a(x, y) &= 0.5(\cos(y) + x(2\pi - x)\sin(x)) + 0.6, \\ b(x, y) &= 2(\cos(y) + \sin(x)) + 0.8. \end{aligned}$$

Data is generated by solving problem (8) using a high precision numerical scheme by discretizing Ω using a 50×50 grid and a time step size $\delta t = 0.015$. We assume periodic boundary condition and the initial value $u_0(x, y)$ is generated from

$$u_0(x, y) = \sum_{|k|, |l| \leq N} \lambda_{k,l} \cos(kx + ly) + \gamma_{k,l} \sin(kx + ly), \quad (9)$$

where $N = 9$, $\lambda_{k,l}, \gamma_{k,l} \sim \mathcal{N}(0, \frac{1}{50})$, and k and l are chosen randomly. We also add noise to the generated data:

$$\tilde{u}(x, y, t) = u(x, y, t) + 0.015 \times MW \quad (10)$$

where $M = \max_{x,y,t} \{u(x, y, t)\}$, $W \sim \mathcal{N}(0, 1)$ and $\mathcal{N}(0, 1)$ represents the standard normal distribution. Details on the data generation and experiments on noise-free case can be found in the supplement (Long et al., 2018).

Suppose we know a priori that the underlying PDE is linear with order no more than 4. Then, the response function F takes the following form

$$F = \sum_{0 \leq i+j \leq 4} f_{ij}(x, y) \frac{\partial^{i+j} u}{\partial x^i \partial y^j}.$$

Each δt -block of the PDE-Net can be written as

$$\begin{aligned} \tilde{u}(t_{n+1}, \cdot) &= D_0 u(t_n, \cdot) \\ &+ \delta t \cdot (c_{00} D_{00} u + c_{10} D_{10} u + \dots + c_{04} D_{04} u), \end{aligned}$$

where $\{D_0, D_{ij} : i + j \leq 4\}$ are convolution operators and $\{c_{ij} : i + j \leq 4\}$ are 2D arrays which approximate functions $f_{ij}(x, y)$ on Ω . The approximation is achieved using piecewise quadratic polynomial interpolation with smooth transitions at the boundaries of each piece. The filters associated to the convolution operators $\{D_0, D_{ij} : i + j \leq 4\}$ and the coefficients of the piecewise quadratic polynomials are the trainable parameters of the network.

During training and testing, the data is generated on-the-fly. The size of the filters that will be used is 5×5 or 7×7 .

The total number of trainable parameters for each δt -block is approximately 17k. During training, we use LBFGS, instead of SGD, to optimize the parameters. We use 28 data samples per batch to train each layer (i.e. δt -block) and we only construct the PDE-Net up to 20 layers, which requires totally 560 data samples per batch.

3.2. Results and Discussions

3.2.1. PREDICTING LONG-TIME DYNAMICS

We first demonstrate the ability of the trained PDE-Net in prediction, which in the language of machine learning is the ability to generalize. After the PDE-Net with n δt -blocks ($1 \leq n \leq 20$) is trained, we randomly generate 560 initial guesses based on (9) and (10), feed them to the PDE-Net, and measure the normalized error between the predicted dynamics (i.e. the output of the PDE-Net) and the actual dynamics (obtained by solving (8) using high precision numerical scheme). The normalized error between the predicted data \tilde{u} and the true data u is defined as $\epsilon = \frac{\|\tilde{u} - u\|_2^2}{\|u - \bar{u}\|_2^2}$, where \bar{u} is the spatial average of u . The error plots are shown in Figure 3. Some of the images of the predicted dynamics are presented in Figure 4.

From these results, we can see that:

- Even trained with noisy data, the PDE-Net is able to perform long-term prediction (see Figure 4);
- Having multiple δt -blocks enables the network to facilitate long-term predictions (see Figure 3);
- The PDE-Net performs significantly better than Frozen-PDE-Net, especially for 7×7 filters (see Figure 3);
- The PDE-Net with 7×7 filters significantly outperforms the PDE-Net with 5×5 filters in terms of the length of reliable predictions (see Figure 3). To reach an $O(1)$ error, the length of prediction for the PDE-Net with 7×7 filters is about 10 times of that for the PDE-Net with 5×5 filters.

3.2.2. DISCOVERING THE HIDDEN EQUATION

For the linear problem, identifying the PDE amounts to finding the coefficients $\{c_{ij} : i + j \leq 4\}$ that approximate $\{f_{ij} : i + j \leq 4\}$. The coefficients $\{c_{ij} : i + j \leq 2\}$ of the trained PDE-Net are shown in Figure 5. Note that $\{f_{11}\} \cup \{f_{ij} : 2 < i + j \leq 4\}$ are absent from the PDE (8), and the corresponding coefficients learned by the PDE-Net are indeed close to zero. In order to have a more concise demonstration of the results, we only show the image of $\{c_{ij} : i + j \leq 2\}$ in Figure 5. Images of all the coefficients are presented in the supplement (Long et al., 2018).

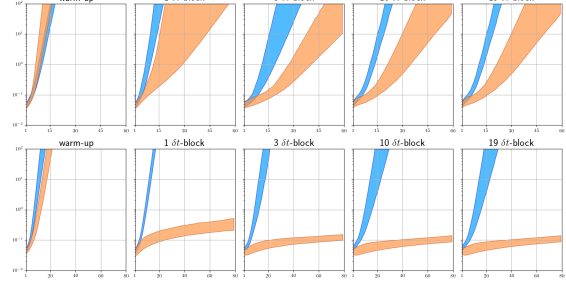


Figure 3. Prediction errors of the PDE-Net (orange) and Frozen-PDE-Net (blue) with 5×5 (first row) and 7×7 (second row) filters. In each plot, the horizontal axis indicates the time of prediction in the interval $(0, 60 \times \delta t] = (0, 0.9]$, and the vertical axis shows the normalized errors. The banded curves indicate the 25% & 75% percentile of the normalized errors among 560 test samples.

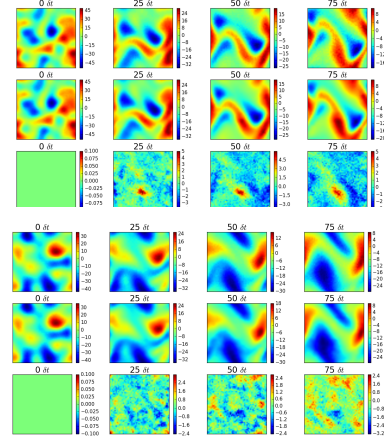


Figure 4. The first row shows the images of the true dynamics. The second row shows the images of the predicted dynamics using the PDE-Net having 3 δt -blocks with 5×5 (up) and 7×7 (down) filters. The third row shows the error maps. Time step $\delta t = 0.015$.

Comparing the first three rows of Figure 5, the coefficients $\{c_{ij}\}$ learned by the PDE-Net are close to the true coefficients $\{f_{ij}\}$ except for some oscillations due to the presence of noise in the training data. Furthermore, the last row of Figure 5 indicates that having multiple δt -blocks helps with estimation of the coefficients. However, having larger filters does not seem to improve the learning of the coefficients, though it helps tremendously in prolonging predictions of the PDE-Net.

3.2.3. FURTHER EXPERIMENTS

The PDE (8) is of second order. In our previous experiments, we assumed that the PDE does not exceed the 4th order. If we know that the PDE is of second order, we will be able to have a more accurate estimation of the variable

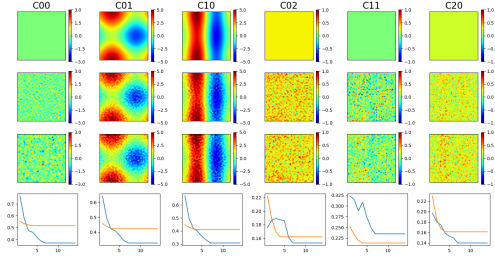


Figure 5. First row: the true coefficients of the equation. From the left to right are coefficients of u , u_x , u_y , u_{xx} , u_{xy} and u_{yy} . Second row: the learned coefficients by the PDE-Net with 6 δt -blocks and 5×5 filters. Third row: the learned coefficients by the PDE-Net with 6 δt -blocks and 7×7 filters. Last row: the errors between true and learned coefficients v.s. number of δt -blocks with different sizes of filters (5×5 blue and 7×7 orange).

coefficients of the convection and diffusion terms. However, the prediction errors are slightly higher since we have fewer trainable parameters. Nonetheless, since we are using a more accurate prior knowledge on the unknown PDE, the variance of the prediction errors are smaller than before. These results are summarized in Figure 6 (green curves) and Figure 7.

To further demonstrate the importance of the moment constraints on the filters in the PDE-Net, we trained the network without any moment constraints. For simplicity, we call the PDE-Net train in this way as the Freed-PDE-Net. The prediction errors of the Freed-PDE-Net are shown as the red curves in Figure 6. Since without moment constraints, we do not know the correspondence of the filters with differential operators. Therefore, we cannot identify the correspondence of the learned variable coefficients either. We plot all the 15 variable coefficients (assuming the underlying PDE is of order ≤ 4) in Figure 8. As one can see that the Freed-PDE-Net is better in prediction than the PDE-Net since it has more trainable parameters than the PDE-Net. However, we are unable to identify the PDE from the Free-PDE-Net. More experiments can be found in the supplement (Long et al., 2018).

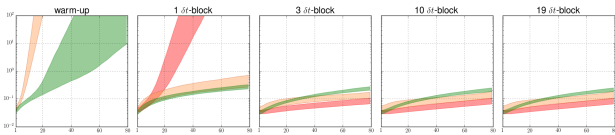


Figure 6. Prediction errors of the PDE-Net assuming the underlying PDE has order ≤ 4 (orange), order ≤ 2 (green) and Freed-PDE-Net (red) with 7×7 filters. In each plot, the horizontal axis indicates the time of prediction in the interval $(0, 80 \times \delta t] = (0, 1.2]$, and the vertical axis shows the normalized errors.

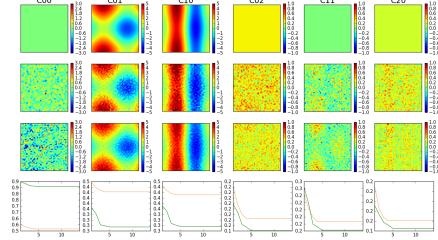


Figure 7. First row: the true coefficients of the equation. From the left to right are coefficients of u , u_x , u_y , u_{xx} , u_{xy} and u_{yy} . Second row: the learned coefficients by the PDE-Net assuming the order of the PDE is ≤ 4 (same as the third row of Figure 5). Third row: the learned coefficients by the PDE-Net assuming the order of the PDE is ≤ 2 . Last row: the errors between true and learned coefficients v.s. number of δt -blocks (1, 2, ..., 13) for PDE-Net assuming the PDE is of order ≤ 4 (orange) and ≤ 2 (green).

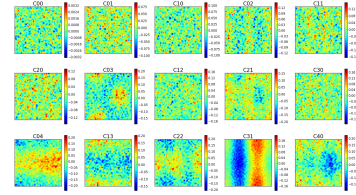


Figure 8. The images of all the variable coefficients learned from the Freed-PDE-Net.

4. Numerical Studies: Diffusion Equations with Nonlinear Source

When modeling physical processes like particle transportation or energy transfer, in addition to convection and diffusion, we have to consider source/sink terms. In some problems, the source/sink plays an important role. For example, when convection-diffusion equations are used to describe the distribution and flow of pollutants in water or atmosphere, identifying the intensity of pollution source is equivalent to finding the source term, which is important for environmental pollution control problems.

4.1. Simulated data, training and testing

We consider a 2-dimensional linear diffusion equation with a nonlinear source on $\Omega = [0, 2\pi] \times [0, 2\pi]$,

$$\begin{cases} \frac{\partial u}{\partial t} = c\Delta u + f_s(u), & \text{with } (t, x, y) \in [0, 0.2] \times \Omega, \\ u|_{t=0} = u_0(x, y), \end{cases} \quad (11)$$

where $c = 0.3$ and $f_s(u) = 15 \sin(u)$. Data is generated similarly as before, except with a time step $\delta t = 0.0009$ and zero boundary condition.

We assume the following form of the response function F

$$F = \sum_{1 \leq i+j \leq 2} f_{ij}(x, y) \frac{\partial^{i+j} u}{\partial x^i \partial y^j} + f_s(u).$$

Each δt -block of the PDE-Net can be written as

$$\tilde{u}(t_{n+1}, \cdot) = D_0 u(t_n, \cdot) + \delta t \cdot \left(\sum_{1 \leq i+j \leq 2} c_{ij} D_{ij} u + \tilde{f}_s(u) \right),$$

where $\{D_0, D_{ij} : 1 \leq i+j \leq 2\}$ are convolution operators and $\{c_{ij} : 1 \leq i+j \leq 2\}$ are 2D arrays which approximate functions $f_{ij}(x, y)$ on Ω . The approximation of \tilde{f}_s is obtained by piecewise 4th order polynomial approximation. The training and testing strategy is exactly the same as in Section 3. In our experiments, the size of the filters is 7×7 . The number of parameters for each δt -block is $\approx 1.2k$.

4.2. Results and Discussions

4.2.1. PREDICTING LONG-TIME DYNAMICS

We first demonstrate the ability of the trained PDE-Net in prediction. The testing method is exactly the same as the method described in Section 3. Comparisons between PDE-Net and Frozen-PDE-Net are shown in Figure 9, where we can clearly see the advantage of learning the filters. Visualization of the predicted dynamics is given in Figure 10. All these results show that the learned PDE-Net performs well in prediction.

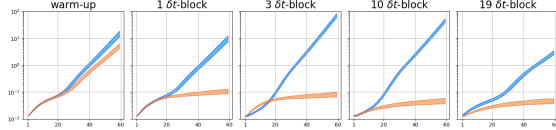


Figure 9. Prediction errors of the PDE-Net (orange) and Frozen-PDE-Net (blue) with 7×7 filters. In each plot, the horizontal axis indicates the time of prediction in the interval $(0, 0.6]$, and the vertical axis shows the normalized errors.

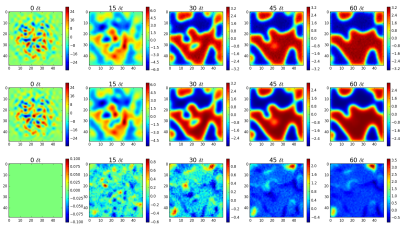


Figure 10. The first row shows the images of the true dynamics. The second row shows the images of the predicted dynamics using the PDE-Net having 3 δt -blocks with 7×7 filters. The third row shows the error maps. Here, $\delta t = 0.01$.

4.2.2. DISCOVERING THE HIDDEN EQUATION

For the PDE (11), identifying the PDE amounts to finding the coefficients $\{c_{ij} : 1 \leq i+j \leq 2\}$ that approximate $\{f_{ij} : 1 \leq i+j \leq 2\}$, and \tilde{f}_s that approximates f_s . The computed coefficients $\{c_{ij} : 1 \leq i+j \leq 2\}$ of the trained PDE-Net are shown in Figure 11, and the computed \tilde{f}_s is shown in Figure 12 (left). Note that the first order terms are absent from the PDE (11), and the corresponding coefficients learned by the PDE-Net are indeed close to zero. The approximation of f_s is more accurate near the center of the interval than near the boundary. This is because the value of u in the data set is mostly distributed near the center (Figure 12(right)).

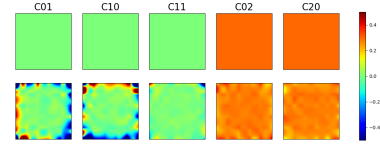


Figure 11. First row: the true coefficients $\{f_{ij} : 1 \leq i+j \leq 2\}$ of the equation. Second row: the learned coefficients $\{c_{ij} : 1 \leq i+j \leq 2\}$ by the PDE-Net with 3 δt -blocks and 7×7 filters.

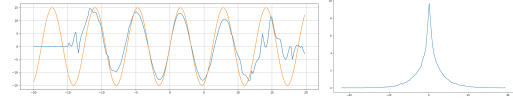


Figure 12. Left: the true source function f_s and estimated source function \tilde{f}_s . Right: distribution of the values of u during training.

5. Conclusion and Discussion

In this paper, we designed a deep feed-forward network, called the PDE-Net, to discover the hidden PDE model from the observed dynamics and to predict the dynamical behavior. The PDE-Net consists of two major components which are jointly trained: to approximate differential operations by convolutions with properly constrained filters, and to approximate the nonlinear response by deep neural networks or other machine learning methods. The PDE-Net is suitable for learning PDEs as general as in (1). As an example, we considered a linear variable-coefficient convection-diffusion equation. The results show that the PDE-Net can uncover the hidden equation of the observed dynamics, and predict the dynamical behavior for a relatively long time, even in a noisy environment. PyTorch codes of the PDE-Net are available at <https://github.com/ZichaoLong/PDE-Net>. As part of the future work, we will try the proposed framework on real data sets. One of the important directions is to uncover hidden variables which cannot be measured by sensors directly, such as in data assimilation. Another interesting direction which is worth exploring is to learn stable and consistent numerical schemes for a given PDE model based on the architecture of the PDE-Net.

Acknowledgments

Bin Dong is supported in part by NSFC 11671022. Zichao Long is supported in part by The National Key Research and Development Program of China 2016YFC0207700. Yiping Lu is supported by the Elite Undergraduate Training Program of the School of Mathematical Sciences at Peking University.

References

- Bongard, Josh and Lipson, Hod. Automated reverse engineering of nonlinear dynamical systems. *Proceedings of the National Academy of Sciences*, 104(24):9943–9948, 2007.
- Brunton, Steven L, Proctor, Joshua L, and Kutz, J Nathan. Discovering governing equations from data by sparse identification of nonlinear dynamical systems. *Proceedings of the National Academy of Sciences*, 113(15):3932–3937, 2016.
- Cai, Jian-Feng, Dong, Bin, Osher, Stanley, and Shen, Zuowei. Image restoration: total variation, wavelet frames, and beyond. *Journal of the American Mathematical Society*, 25(4):1033–1089, 2012.
- Chandrasekhar, Subrahmanyan. Stochastic problems in physics and astronomy. *Reviews of modern physics*, 15(1):1, 1943.
- Chang, Bo, Meng, Lili, Haber, Eldad, Tung, Frederick, and Begert, David. Multi-level residual networks from dynamical systems view. In *ICLR*, 2018.
- Chen, Yunjin, Yu, Wei, and Pock, Thomas. On learning optimized reaction diffusion processes for effective image restoration. In *Proceedings of the IEEE Conference on Computer Vision and Pattern Recognition*, pp. 5261–5269, 2015.
- Daubechies, Ingrid. *Ten lectures on wavelets*. SIAM, 1992.
- de Bezenac, Emmanuel, Pajot, Arthur, and Gallinari, Patrick. Deep learning for physical processes: Incorporating prior scientific knowledge. *arXiv preprint arXiv:1711.07970*, 2017.
- Dong, Bin, Jiang, Qingtang, and Shen, Zuowei. Image restoration: wavelet frame shrinkage, nonlinear evolution pdes, and beyond. *Multiscale Modeling & Simulation*, 15(1):606–660, 2017.
- E, Weinan. A proposal on machine learning via dynamical systems. *Communications in Mathematics and Statistics*, 5(1):1–11, 2017.
- Haber, Eldad and Ruthotto, Lars. Stable architectures for deep neural networks. *arXiv preprint arXiv:1705.03341*, 2017.
- He, Kaiming, Zhang, Xiangyu, Ren, Shaoqing, and Sun, Jian. Deep residual learning for image recognition. In *Proceedings of the IEEE conference on computer vision and pattern recognition*, pp. 770–778, 2016a.
- He, Kaiming, Zhang, Xiangyu, Ren, Shaoqing, and Sun, Jian. Identity mappings in deep residual networks. In *European Conference on Computer Vision*, pp. 630–645. Springer, 2016b.
- Lin, Min, Chen, Qiang, and Yan, Shuicheng. Network in network. *arXiv preprint arXiv:1312.4400*, 2013.
- Long, Zichao, Lu, Yiping, Ma, Xianzhong, and Dong, Bin. Supplementary material., 2018. URL <http://bicmr.pku.edu.cn/~dongbin/Publications/PDE-Net-SuppMat.pdf>.
- Lu, Yiping, Zhong, Aoxiao, Li, Quanzheng, and Dong, Bin. Beyond finite layer neural networks: Bridging deep architectures and numerical differential equations. *ICML*, 2018.
- Mallat, Stéphane. *A wavelet tour of signal processing*. Academic press, 1999.
- Raissi, Maziar and Karniadakis, George Em. Hidden physics models: Machine learning of nonlinear partial differential equations. *arXiv preprint arXiv:1708.00588*, 2017.
- Raissi, Maziar, Perdikaris, Paris, and Karniadakis, George Em. Physics informed deep learning (part ii): Data-driven discovery of nonlinear partial differential equations. *arXiv preprint arXiv:1711.10566*, 2017.
- Rudy, Samuel H, Brunton, Steven L, Proctor, Joshua L, and Kutz, J Nathan. Data-driven discovery of partial differential equations. *Science Advances*, 3(4):e1602614, 2017.
- Schaeffer, Hayden. Learning partial differential equations via data discovery and sparse optimization. In *Proc. R. Soc. A*, volume 473, pp. 20160446. The Royal Society, 2017.
- Schmidt, M and Lipson, H. Distilling free-form natural laws from experimental data. *Science (New York, N.Y.)*, 324(5923):81–5, 2009.
- Sonoda, Sho and Murata, Noboru. Double continuum limit of deep neural networks. *ICML Workshop on Principled Approaches to Deep Learning*, Sydney, Australia, 2017.
- Wu, Zongmin and Zhang, Ran. Learning physics by data for the motion of a sphere falling in a non-newtonian fluid non-newtonian fluid. *preprint*, 2017.